A step towards measuring connectivity in the deep-sea: elemental fingerprints of mollusk larval shells discriminate hydrothermal sites

Vincent Mouchi[1], Christophe Pecheyran[2], Fanny Claverie[2], Cécile Cathalot[3], Marjolaine Matabos[4], Olivier Rouxel[3], Didier Jollivet[1], Thomas Broquet[1], Thierry Comtet[1]

[1]: Sorbonne Université, Adaptation et Diversité en Milieu Marin, UMR 7144, Station Biologique de Roscoff, F-29680, Roscoff, France

[2] : Université de Pau et des Pays de l'Adour/CNRS, Institut des Sciences Analytiques et de Physico-Chimie pour l’Environnement et les Matériaux, UMR 5254, F-64053, Pau, France

[3]: IFREMER REM-GM, Technopôle Brest Plouzané, 29280 Plouzané, France

[4]: IFREMER REM-EEP, Technopôle Brest Plouzané, 29280 Plouzané, France

ABSTRACT

Deep-sea hydrothermal vent systems are under investigation for metal and rare earth element exploitations. The negative impacts on natural and endemic populations in these areas are still unclear. Larval dispersal is critical for colonization and settlements of populations in marine environments, and assessing connectivity is challenging, especially in deep-sea environments. Here, we investigate the potential of elemental fingerprinting of mollusc larval shells to discriminate larvae origins between multiple hydrothermal sites in the Southwest Pacific Ocean. We identified the gastropod *Shinkailepas tollmanni* as a suitable candidate as this species uses capsules to hold larvae before dispersal, which facilitates sampling. Cutting-edge femto-second laser ablation was performed to obtain individual measurements on 600 larval shells. We used classification methods to discriminate the origin of these individuals from 14 sampled hydrothermal sites across 3,500 km, with an overall success rate of 70%. When considering less sites within a more restricted area, reflecting dispersal distances inferred from genetic or modelling approaches, we increase the success rate up to 86%. We conclude that elemental fingerprinting is a suitable method to assess connectivity from hydrothermal vent populations, and that the measurements of preserved larval shells in juvenile individuals (*i.e.*, those who completed dispersal) can give reliable information on their geographic origin.

INTRODUCTION

Deep-sea hydrothermal vent systems induce the formation of massive polymetallic sulphide deposits from the ascent and circulation of hydrothermal fluids enriched in heavy elements in the oceanic crust (*e.g.*, Fouquet et al., 1991). The presence of such deposits in contexts of tectonic collision and spreading have suggested that hydrothermal vent fields could be economically-viable metal and rare earth element exploitation areas. Mining initiatives are currently under evaluation in multiple regions of the world (Boschen et al., 2013; Dunn et al., 2018), to reach more than 1.4 million km² of the seabed affected in areas beyond national jurisdiction (Jouffray et al., 2020). Deep-sea mining activities are expected to strongly disturb hydrothermal vent ecosystems and their vicinity in the targeted vent fields (Danovaro et al., 2017, 2020), yet very little is known on the resilience of vent communities that constitute biomass hotspots in the deep-sea (Dunn et al., 2018; Suzuki et al., 2018). Over the past decade, numerous studies have highlighted the lack of knowledge needed to assess the potential impacts of deep-sea mining and to implement mitigation and protection measures (*e.g.*, Van Dover, 2014; Gollner et al., 2017; Miller et al., 2018; Smith et al., 2020; Christiansen et al., 2022; Amon et al., 2022). In particular, population connectivity has been identified as a key scientific knowledge gap, including in the well-studied hydrothermal vent ecosystems (Gollner et al., 2017; Miller et al., 2018; Smith et al., 2020; Amon et al. 2022).

Hydrothermal vent fields are ephemeral, patchy habitats, separated by hundreds to thousands of kilometres. The resilience of the populations that are associated with these habitats depends critically on their connectivity, *i.e.*, the exchange of individuals within and across active hydrothermal vent sites. For many benthic vent species, pelagic larvae are the major, if not the only vector of dispersal between populations in multiple vent sites, as well as the only, vector of colonization of new sites. Accurately estimating larval dispersal is therefore critical to our understanding of the demographic trajectory of hydrothermal metapopulations, especially in the context of deep-sea mining (*e.g.*, Amon et al., 2022). It is however extremely difficult to catch minute-sized larvae released at great depths, and it is impossible to track directly their journey between their point of release and their settlement location as they follow underwater currents. Indirect inference methods are therefore required.

Biophysical models use physical oceanographic data and species-specific biologic features, such as the planktonic larval duration (PLD) and potential behaviours (*e.g.*, vertical migration), to estimate the spatial extent of larval transport in a given geographic area (*e.g.*, Mitarai et al., 2016; Yearsley et al. 2020). However, biological and hydrodynamic parameters are hardly constrained, inducing uncertainties in the distance and direction larvae travel (*e.g.*, McVeigh et al. 2017). Another class of methods use population genetics to infer migration between populations (Baco et al. 2016; Breusing et al. 2016; Tran Lu Y et al., 2022). Genetic methods, however, are limited in many marine invertebrates because large populations experience weak genetic drift and therefore weak genetic structure regardless of migration rates (Gagnaire et al., 2015). Even when genetic structure is strong enough, it remains difficult to infer gene flow and translate it into demographic connectivity parameters. Genetic methods also use more direct approaches, *e.g.*, based on parentage analyses, but these are applicable only when a very significant fraction of individuals can be sampled (Gagnaire et al., 2015), which in effect happens in only very particular systems, and certainly not in the deep-sea.

Surprisingly, although it has been proposed for many years as a tool to study larval dispersal (Levin, 1990; Levin et al., 1993), and has been widely used in coastal environments (Zacherl et al., 2003; Becker et al., 2005, 2007; Carson, 2010; Fodrie et al., 2011; Kroll et al., 2016; Honig et al., 2020; Bounket et al., 2021), the alternative approach of elemental fingerprinting of biogenic carbonate structures (such as otoliths or shells) has never been used in deep-sea species (Baco et al., 2016; Cunha et al., 2020). The success of this approach relies on the record in calcified structures of the chemical composition of the water in which they have been built (*e.g.*, Thorrold et al. 2007). When differences exist in the chemical composition of seawater between various locations, they can be recorded in the calcified structures of organisms living there, although environmental conditions (*e.g.*, temperature; Thorrold et al. 2007) and metabolism (*e.g.*, Mouchi et al., 2020) have been reported to modify the exact seawater composition reflection in biominerals. In species that produce calcified structures at the larval stage, like fish (otoliths) or molluscs (shells), the elemental fingerprint of the larval structure preserved in later developmental stages therefore allows for the determination of their natal geographic origin, provided that the larval calcified structures have been built in sites with differing compositions (Becker et al., 2007; Thorrold et al., 2007). Although never attempted in the deep-sea, this approach sounds promising in hydrothermal vent systems as different chemical compositions are expected at various spatial scales. Besides, the development of new cutting-edge analytical methods now allows precise geochemical measurements on individual minute-size larval shells.

A first deep-sea mining licence has been allocated to extract metals in the South-western Pacific, in the Manus Basin, offshore Papua New Guinea, at Solwara 1 (Gwyther, 2008). In order to properly address its potential future impact on neighbouring ecosystems, a scientific cruise (Hourdez & Jollivet, 2019) collected living specimens from a variety of species at multiple hydrothermal vent sites across 3,500 km in the Southwest Pacific in 2019 (**Fig. 1**). Our study focuses on the elemental fingerprint of larval shells of the gastropod *Shinkailepas tollmanni* (L. Beck, 1992), to evaluate for the first time the potential of elemental fingerprinting in deep-sea hydrothermal vent systems for connectivity assessment. *Shinkailepas* is an abundant species endemic to hydrothermal vents and females lay eggs on shells of the large gastropod *Ifremeria nautilei* (**Fig. 2**). The key feature of this species is that it lays capsules within which eggs develop into shelled veliger larvae before their release in the water column. It means that the encapsulated larval carbonate shell incorporates chemical elements present in the surrounding seawater from the vent environment before starting to disperse. We here aimed to determine whether the elemental composition of encapsulated larval shells records a distinct chemical signature between populations, which is the first necessary step towards using elemental fingerprinting to estimate connectivity between sites. The challenge is the minute size of the encapsulated larval shells (**Fig. 2f**) which requires cutting-edge analytical method to perform high-quality geochemical measurements to highlight potential discriminating composition between sites of origin. We analysed a total of 600 larvae collected from 14 sites in the South-western Pacific, together with water samples taken in close proximity to the egg capsules.

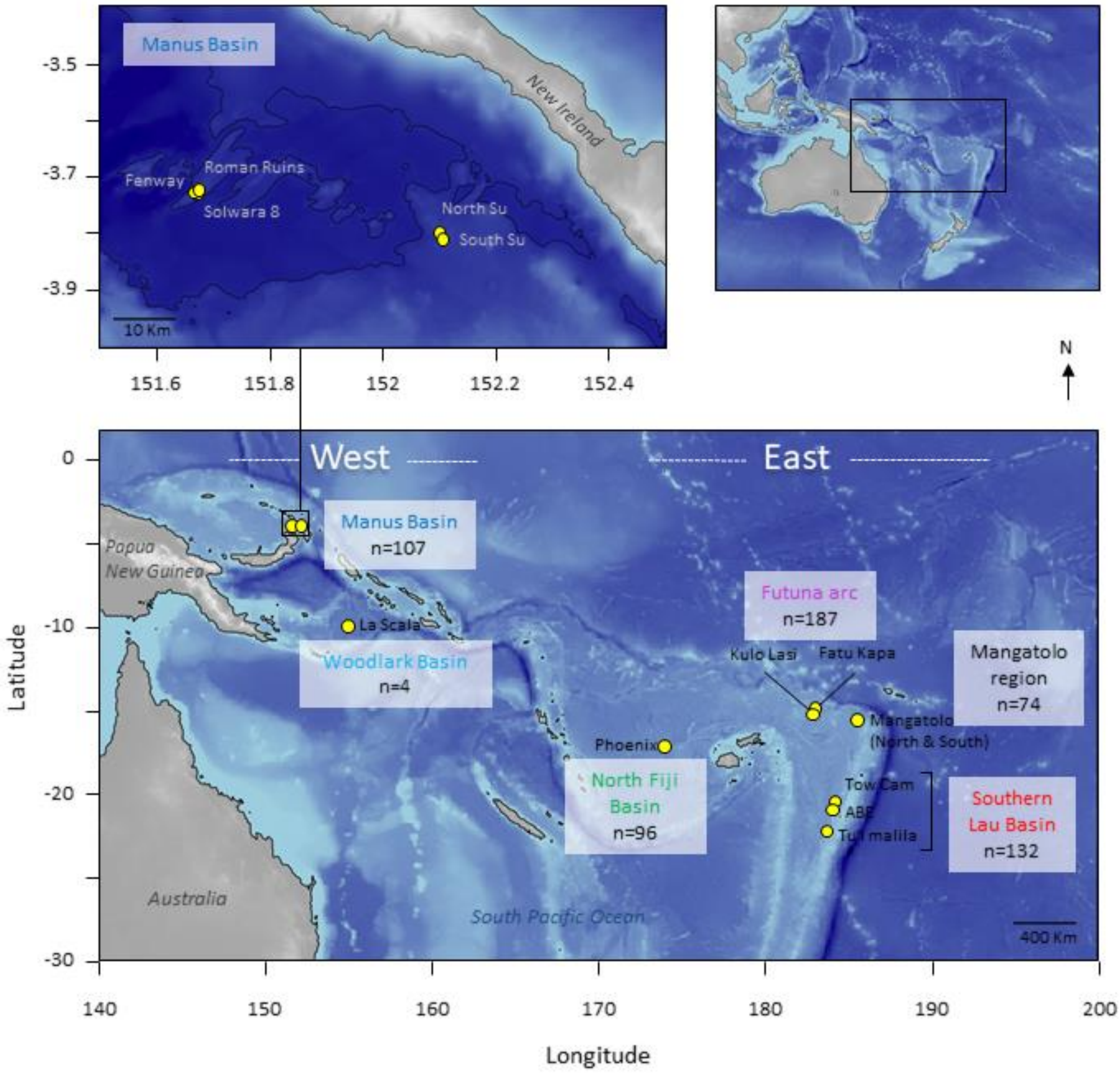

Figure 1: Map of the Southwest Pacific locating samples. The number of specimens is indicated for each region. Although Mangatolo is located in the Lau Basin, we decided to consider it as a separate region due to its distance with the other Lau sites.

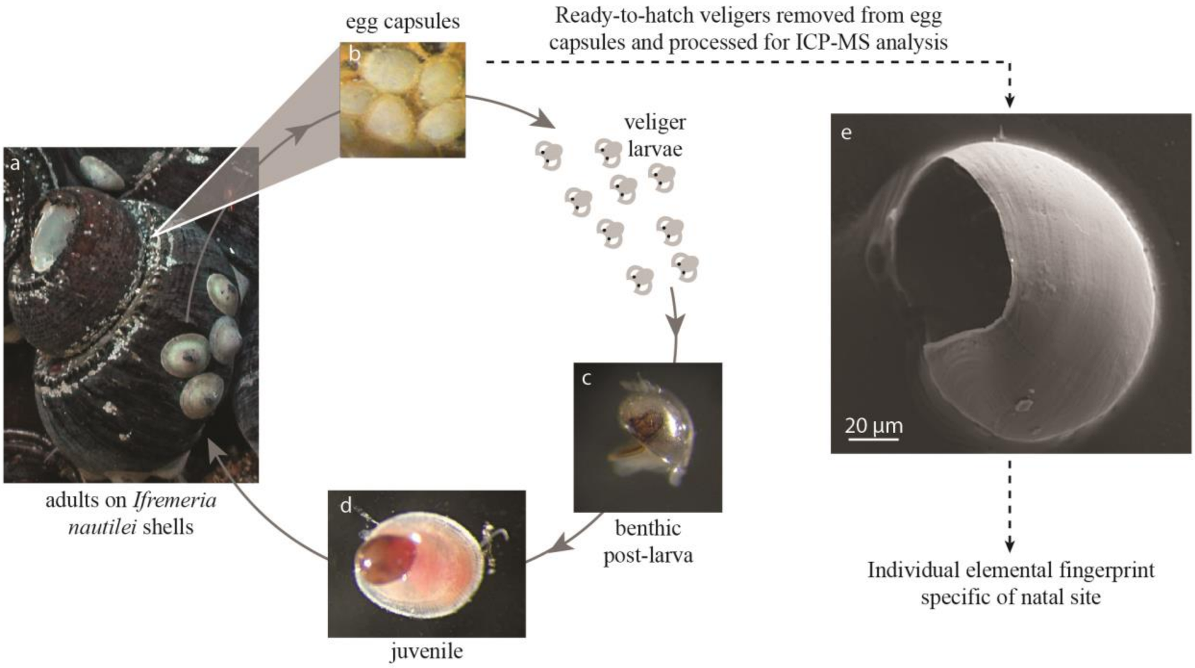

Figure 2: Life cycle of *Shinkailepas tollmanni*. *Ifremeria nautilei* (**a**) shell grooves serve as depository of *S. tollmanni* egg-capsules (**b**) which hold encapsulated larvae. When the capsules open, the shelled larvae disperse in seawater until metamorphosis when the individual reaches a hydrothermal site (recruitment; **c**). The new recruit grows a juvenile shell while preserving its larval shell (**d**). A scanning electron microscope picture of an encapsulated larval shell (**e**) is presented (secondary electron mode, 15kV).

RESULTS and DISCUSSION

Seawater composition

Ifremeria communities (and thus *S. tollmanni*) are found in the vent diffusion zone, as illustrated by the recorded temperature range of approximately 30°C in their habitat (Podowski et al., 2010). Thus, *S. tollmanni* is in contact with a mixture of seawater and the hydrothermal fluid, which proportion will vary depending on the vent activity. This mixture will hereafter be referred to as the ‘habitat seawater’. We investigated the potential differences found in the habitat seawater composition at the level of these communities, which may be caused by the geologic nature of sediments and substrate.

Habitat seawater composition differed among only some of the sampled sites (**Fig. 3** and **Supplementary Information 1**). Principal Component Analysis (PCA) from 40 samples and 19 elements explained 65.8% of the total variance on three axes. The difference between sites was particularly obvious for the Mangatolo site, which was identified on PCA 1 and 3 (**Fig. 3**). The habitat seawater samples collected on two close chimneys at Fatu Kapa (Futuna), Aster’X and Stéphanie, were also isolated from the rest of the samples and carried on PCA 3. However, habitat seawater from other localities presented more overlap, especially in the western domain (blue symbols in **Figure 3**).

These results indicated that the chemical composition of the habitat seawater presented some variability able to, at least to some geographic scale, discriminate between sites. Still, as metabolism can change the fluid composition recorded in the shell, *S. tollmanni* elemental fingerprints remained to be evaluated in order to validate this method as a tool for origin determination.

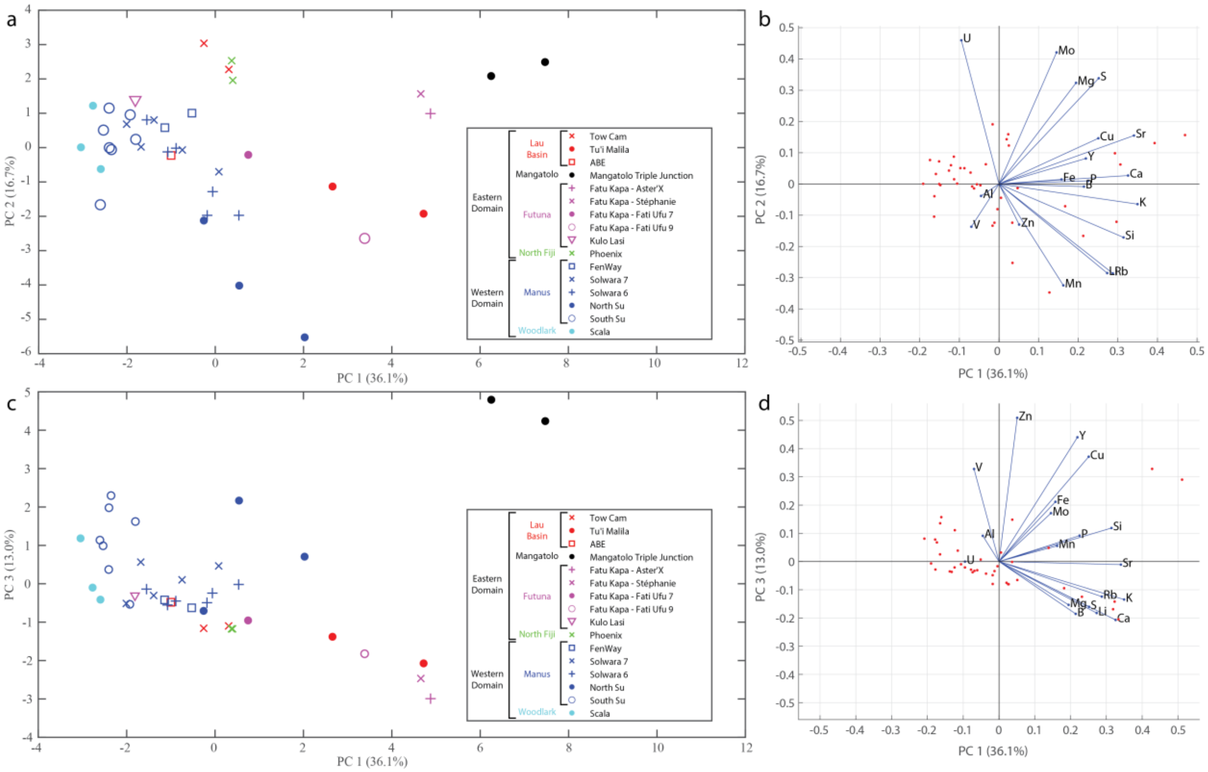

Figure 3: Principal Component Analysis of habitat seawater compositions collected over the *Ifremeria* communities on sample sites, showing projections on components 1 and 2 (**a** and **b**) and 1 and 3 (**c** and **d**). The legend gathers all sites by region (Lau Basin, Mangatolo, Futuna, North Fiji, Manus and Woodlark) and by domain (East and West).

Chemical composition of Shinkailepas tollmanni *encapsulated larval shells*

The gyroscopic femtosecond laser ablation system coupled with a triple-quadrupole ICP-MS allowed the measurements of 14 elements from 600 encapsulated larval shells of *S. tollmanni* despite their minute size (100 µm empty spheres, approx. 2 µm thickness; **Fig. 2f**). Measured abundances (**Supplementary Information 2**) ranged from 0.5 ppb (for Sb) to 10.2 10^3 ppm (for Mg).

Contrary to the habitat seawater data presented above, PCA results of larval shell composition did not exhibit any obvious geographic clustering (**Fig. 4**), with 45.5% of the total variance expressed on three axes. Principal Component 1 did not appear to hold geographic information. The main separation of regional samples was carried out on PC 2 by Mn and Ba, with shells from Futuna, Mangatolo and Manus generally exhibiting lower abundances of these elements compared to those of the other regions. Although promising for habitat seawater concentrations, PCA appeared as inadequate to explore potential elemental fingerprints of larval shells.

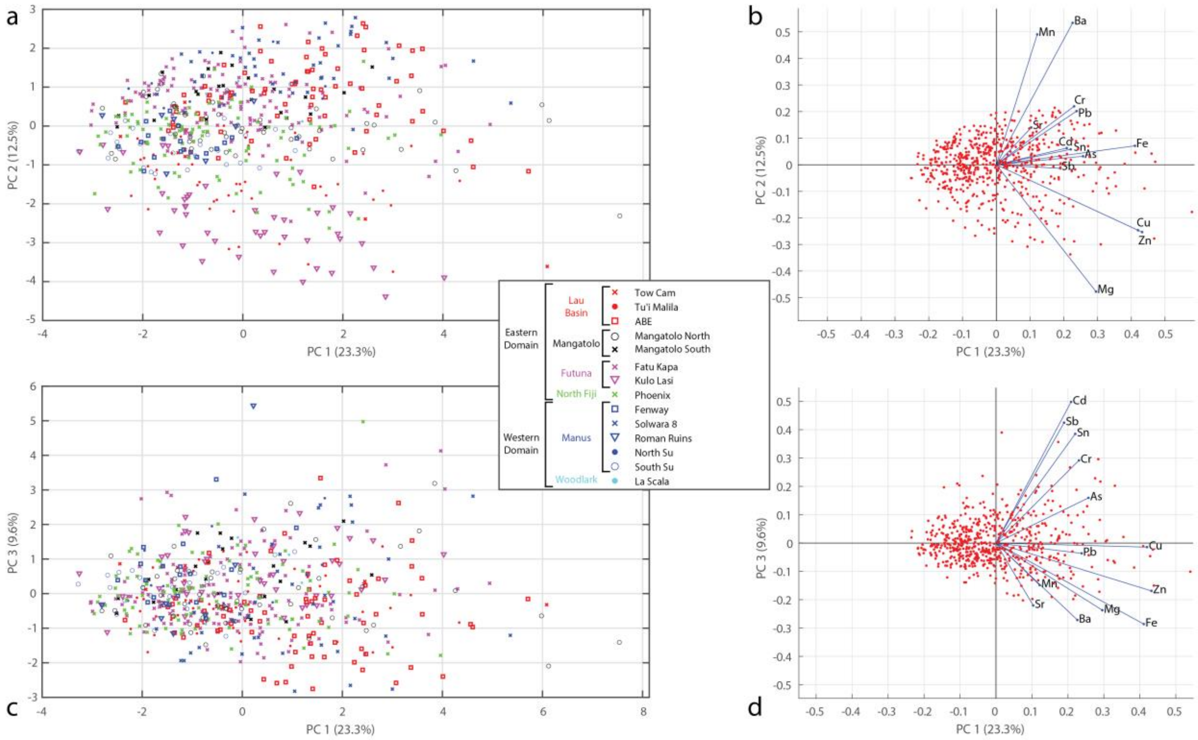

Figure 4: Principal Component Analysis of larval shell compositions for three axes, showing projections on components 1 and 2 (**a** and **b**) and 1 and 3 (**c** and **d**). The variance explained by each principal component is given in parentheses.

Looking into more details at the variation of each element (**Supplementary Information 3**), no single element or pair of elements seemed able to discriminate all sites of origin, although some sites can be substantially different in their composition compared to all other sites. This was particularly visible for Kulo Lasi where larval shells presented strongly depleted abundance in Mn. Other elements, namely Mg, Fe, Zn, Ba and Pb, presented a clear variability between sites, but values systematically overlapped for several sites, even across distant regions. The rest of the measured elements appeared to have low geographic influence. For Cr, As, Cd and Sb, the apparent homogeneity between sites was probably due to their extremely low abundances in shells (generally in the range 1-10 ppm; **Supplementary Information 2**), and represented the limit of the analytical method. Copper presented slightly higher abundances, between 0.7 and 643.5 ppm (**Supplementary Information 2**). Interestingly, Cu was the metal exhibiting the lowest concentration in the *Ifremeria* community seawater (**Supplementary Information 1**).

As we suspected, element concentrations in habitat seawater appeared to be poor predictors of the concentrations in larval shells. This could be monitored for six elements that were measured both in habitat seawater and the encapsulated larval shells (Mg, Mn, Fe, Cu, Zn, and Sr). Among these elements, we used Mn as a dilution factor proxy for hydrothermal fluids in seawater, and performed comparison between habitat seawater measurements and shell abundances from Mn ratios. We noted only a weak but significant positive correlation ($r^2 = 0.43$-0.64, *p-value* < 0.001) for Mg/Mn, Cu/Mn, Zn/Mn and Sr/Mn, while Fe/Mn presented no significant correlation (**Supplementary Information 4**). This difference in composition had already been observed and was probably due to vital effects (Weiner & Dove, 2003; Ulrich et al., 2021) induced by the metabolic filter between surrounding seawater and shell carbonate. Several factors can be at play to cause this difference. Firstly, *S. tollmanni* larval shells are formed in capsules laid by the adult females and are filled with a fluid of undefined composition. It is still unclear if this fluid is directly sampled from the surrounding seawater, or at least partially derived from it in the adult body. Moreover, no information is available on the structure of these capsules, in particular its permeability, that could allow some chemical elements to exchange between the capsule fluid and the environment during larval development. Secondly, metabolic activity requires elements from the environment to operate in all types of settings. Indeed, Zn is used as a co-factor of carbonic anhydrase in Zn-depleted conditions by diatoms (Lee et al., 1995). Also, Cd can be used by methanotrophic archaea as a co-factor of methanol dehydrogenase (Pol et al., 2014). The metabolic use of chemical elements hampers their incorporation in the shell. Another reason for the difference in composition is that the shell is formed by a fluid derived from the external seawater in a compartment between the body and the calcifying carbonate, as the chemistry of this fluid is controlled by the larva (Ramesh et al., 2017). It has been demonstrated that organisms are able to change the pH of this fluid to increase calcification rate (Ramesh et al., 2017), which in turn favours Ca substitutions with other metals (Watson, 2004; DePaolo, 2011; Ulrich et al., 2021). Last but not least, mineralogy is also responsible for the selection of some elements over others in the carbonate lattice because of their atomic radii and charges. For instance, Sr presents a 10 fold higher incorporation coefficient in aragonite compared to calcite. For all these reasons, expecting a similar composition in seawater and shell carbonate is hazardous, as is suggested by our data. We conclude that it is not possible to use the chemical contrasts observed in habitat seawater between sites as reliable predictors of the shell chemistry for origin assignation of individuals, as noted in fish otoliths (Bouchoucha et al., 2018). However, although the biological filter influencing shell construction modifies the chemical assemblage from habitat seawater, elemental fingerprints of shell carbonates may still be specific to some geographic areas and provide information on connectivity of hydrothermal vent species.

Elemental fingerprints of larval shells

Although linear discriminant analysis of elemental fingerprints has been used to assess connectivity in coastal environments (*e.g.*, Becker et al., 2005; Gomes et al., 2006), it was demonstrated that this method is often not the most accurate (Dixon & Brereton, 2009; Mercier et al., 2011). We applied 31 classification methods on the geochemical measurements from the encapsulated larval shells in order to identify the best fitting model to determine their geographical origin. For each dataset considered below, we performed all models successively with a different number and combination of elements, in order to reduce the noise added by irrelevant predictors, as suggested by Mercier et al. (2011).

When considering all sites, the best results were obtained by Quadratic Support Vector Machines using Mg, Mn, Fe, Zn, Sr, Ba, and Pb as predictors (**Fig. 5**), with a 70.0% mean accuracy. With this model, correct assignation of the site ranged from 25% for La Scala to 93.5% for Kulo Lasi (Futuna). The weak assignation success at La Scala may be due to the low amount of specimens from this location (n=4). The composition of shells from Kulo Lasi was well identified by the low abundance in Mn (**Supplementary Information 3**; also visible in habitat seawater: see **Supplementary Information 1**), which explains the high classification success of this group. Kulo Lasi is known to be characterized by significant differences in hydrothermal fluid composition as well as mineralizations compared to other hydrothermal systems (Fouquet et al., 2018; Konn et al., 2018). This implies that if larval dispersal occurs from Kulo Lasi, their origin could be identified simply by Mn abundance measurements from the larval shell of juveniles collected on any site.

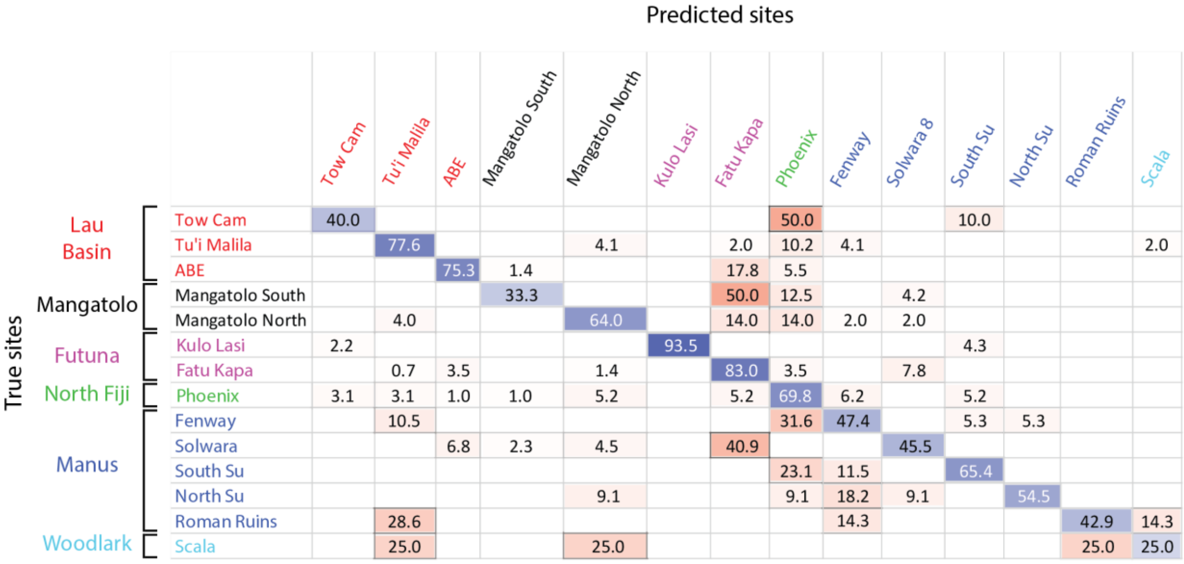

Predicted sites

True sites

		Tow Cam	Tu'i Malila	ABE	Mangatolo South	Mangatolo North	Kulo Lasi	Fatu Kapa	Phoenix	Fenway	Solwara 8	South Su	North Su	Roman Ruins	Scala
Lau Basin	Tow Cam	40.0							50.0			10.0			
	Tu'i Malila		77.6			4.1		2.0	10.2	4.1					2.0
	ABE			75.3	1.4			17.8	5.5						
Mangatolo	Mangatolo South				33.3			50.0	12.5		4.2				
	Mangatolo North		4.0			64.0		14.0	14.0	2.0	2.0				
Futuna	Kulo Lasi	2.2					93.5					4.3			
	Fatu Kapa		0.7	3.5		1.4		83.0	3.5		7.8				
North Fiji	Phoenix	3.1	3.1	1.0	1.0	5.2		5.2	69.8	6.2		5.2			
Manus	Fenway		10.5						31.6	47.4		5.3	5.3		
	Solwara			6.8	2.3	4.5		40.9			45.5				
	South Su								23.1	11.5		65.4			
	North Su					9.1			9.1	18.2	9.1		54.5		
	Roman Ruins		28.6							14.3				42.9	14.3
Woodlark	Scala		25.0			25.0								25.0	25.0

Figure 5: Confusion matrix of the classification of *S. tollmanni* larval shell geochemistry between all sites, in percentage of correct assignation (in blue) and wrong assignation (in red) for each line (corresponding to one site). This classification was made using Quadratic Support Vector Machines, reaching an overall 70.0% accuracy.

From all sites, Phoenix (North Fiji) appeared to present the most heterogeneity in larval shell composition, and numerous larvae from other sites were wrongly assigned to this location. Similarly, nearly a third of the larvae from Phoenix were assigned to other locations by the model (69.8% accuracy for Phoenix). This heterogeneity was not explained by any single element (see boxplots in **Supplementary Information 3**). Overall, an assignation by the model to Phoenix as the origin of a *S. tollmanni* individual should be accepted with caution.

The success rate of this model was largely superior to random chance (20.1%, using randomization; $p < 0.002$). Still, the success rate can improve even more when additional geographic information can be provided by other methods such as biophysical models or population genetics. Biophysical models suggest that the Eastern regions (North Fiji, Futuna, Lau and Mangatolo) and Manus have no direct connectivity, and that Woodlark acts as a sink region for both ensembles (Matarai et al., 2016). Moreover, recent genetic data on several gastropod species also reported limited migration between the Eastern and Western domains (Castel et al., 2022; Tran Lu Y et al., 2022), and that Woodlark could act as a 'stepping stone' in the dispersal of *S. tollmanni* and other species (Poitrimol et al., 2022). In particular, Tran Lu Y (2022, p. 91) identified a strong genetic break between *S. tollmanni* populations indicating a complete absence of dispersal between the Manus basin and any site from the Eastern domain, while the two diverging *S. tollmanni* populations coexist (without admixture) at Woodlark site La Scala. Based on these results, we can refine our previous model consisting of the 14 hydrothermal vent sites. A new series of models was therefore evaluated to study the western domain, focusing on all Manus and Woodlark basin sites as potential origins. The accuracy reached 86.5% by Trilayered Neural Network, using Mn and Ba as predictors (**Fig. 6a**), compared to 26.1% by random chance ($p<0.001$). Site accuracy ranged from 54.5% for North Su to 100% for Solwara 8. Similarly, the best fitting model for the Eastern sites with Woodlark presented an accuracy of 77.1% and was performed by Quadratic SVM with Mg, Mn, Fe, Zn, Sr, Ba and Pb as predictors (**Fig. 6c**), compared to 23.7% by chance ($p<0.001$). This model presented a better accuracy than the one obtained to identify the region of origin from the same dataset (Eastern Domain and Woodlark; **Fig. 6b**) by the same method and predictors, with 75.3%, while chance alone reached 35.3% ($p<0.001$). This small improved quality of the site model may be due to the strong difference in Mn abundance between the sites from Futuna (Kulo Lasi and Fatu Kapa) that are considered as one single class by the region model.

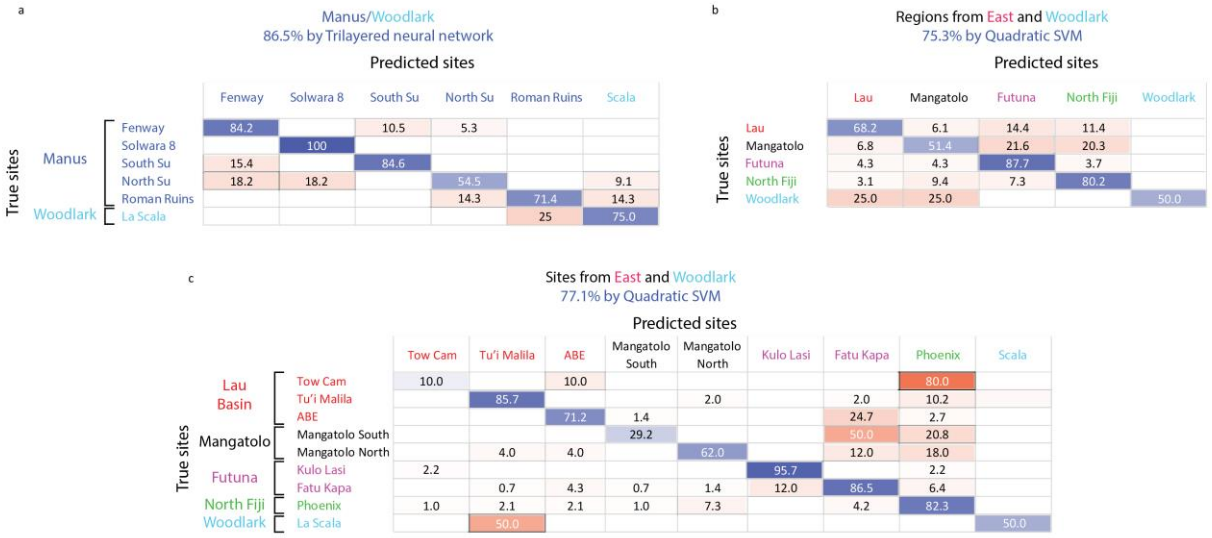

a

Manus/Woodlark
86.5% by Trilayered neural network

Predicted sites

True sites		Fenway	Solwara 8	South Su	North Su	Roman Ruins	Scala
Manus	Fenway	84.2		10.5	5.3		
	Solwara 8		100				
	South Su	15.4		84.6			
	North Su	18.2	18.2		54.5		9.1
	Roman Ruins				14.3	71.4	14.3
Woodlark	La Scala					25	75.0

b

Regions from East and Woodlark
75.3% by Quadratic SVM

Predicted sites

True sites	Lau	Mangatolo	Futuna	North Fiji	Woodlark
Lau	68.2	6.1	14.4	11.4	
Mangatolo	6.8	51.4	21.6	20.3	
Futuna	4.3	4.3	87.7	3.7	
North Fiji	3.1	9.4	7.3	80.2	
Woodlark	25.0	25.0			50.0

c

Sites from East and Woodlark
77.1% by Quadratic SVM

Predicted sites

True sites		Tow Cam	Tu'i Malila	ABE	Mangatolo South	Mangatolo North	Kulo Lasi	Fatu Kapa	Phoenix	Scala
Lau Basin	Tow Cam	10.0		10.0					80.0	
	Tu'i Malila		85.7			2.0		2.0	10.2	
	ABE			71.2	1.4			24.7	2.7	
Mangatolo	Mangatolo South				29.2			50.0	20.8	
	Mangatolo North		4.0	4.0		62.0		12.0	18.0	
Futuna	Kulo Lasi	2.2					95.7		2.2	
	Fatu Kapa		0.7	4.3	0.7	1.4	12.0	86.5	6.4	
North Fiji	Phoenix	1.0	2.1	2.1	1.0	7.3		4.2	82.3	
Woodlark	La Scala		50.0							50.0

Figure 6: Confusion matrices of the classification of *S. tollmanni* larval shell geochemistry within domains with Woodlark region. **a:** Between sites only from Manus and Woodlark basins, using Mn and Ba as predictors. **b:** Between regions only from Futuna volcanic arc and Woodlark, North Fiji, Lau, and Mangatolo basins, using Mg, Mn, Fe, Zn, Sr, Ba and Pb as predictors. **c:** Between sites only from Futuna volcanic arc and Woodlark, North Fiji, Lau, and Mangatolo basins, using Mg, Mn, Fe, Zn, Sr, Ba and Pb as predictors.

In the future, if additional external information points to more locally-restricted dispersal, the assignation success would increase on the Eastern Domain. Indeed, if we consider dispersal to be limited to a single basin, precision of assignation to the site reaches 97.3%, 97.7% and 100% for Mangatolo, Lau Basin, and Futuna, respectively (**Fig. 7**), while chance alone success rate would be 65.4% ($p<0.001$), 53.7% ($p<0.001$), and 75.4% ($p<0.001$), respectively. The elements that were kept as predictors were Ba for all regions, as well as Fe for Mangatolo and Mn for Lau and Futuna.

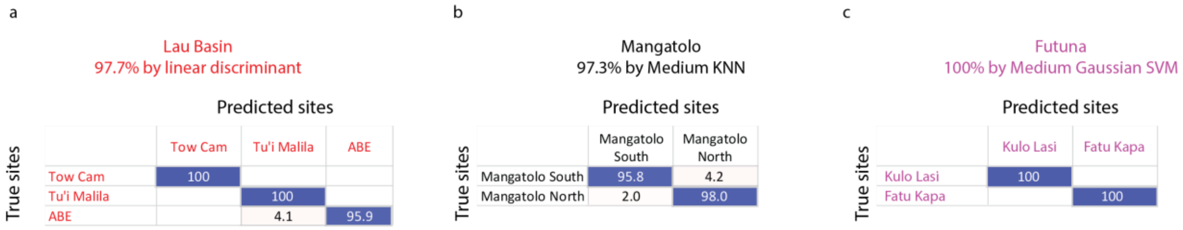

a

Lau Basin
97.7% by linear discriminant

Predicted sites

True sites	Tow Cam	Tu'i Malila	ABE
Tow Cam	100		
Tu'i Malila		100	
ABE		4.1	95.9

b

Mangatolo
97.3% by Medium KNN

Predicted sites

True sites	Mangatolo South	Mangatolo North
Mangatolo South	95.8	4.2
Mangatolo North	2.0	98.0

c

Futuna
100% by Medium Gaussian SVM

Predicted sites

True sites	Kulo Lasi	Fatu Kapa
Kulo Lasi	100	
Fatu Kapa		100

Figure 7: Confusion matrices of the classification of *S. tollmanni* larval shell geochemistry between sites for each Eastern region (**a**: Lau Basin; **b**: Mangatolo; **c**: Futuna volcanic arc), in percentage of correct assignation (in blue) and wrong assignation (in red) for each line (corresponding to one site). For each matrix, the precision and type of model are indicated. The elements kept to build these models are Mn and Ba for Lau Basin and Futuna volcanic arc, and Fe and Ba for Mangatolo.

Our results are in accordance with Mercier et al. (2011) regarding the necessity of selection of elements used for classification; all predictors had different impact on the determination of origin, and some had a negative impact, in particular elements with generally low values that tended to induce noise rather than signal in the discrimination. This was the case here for Cr, As, Cd, Sb, and to a lesser extent, Cu and Sn. Removing these elements systematically improved the validation of all models. In other words, a large number of predictors did not provide a better quality discrimination model: using all 13 available elements, classification procedures for all sites using 31 methods presented assignation success rates ranging from 24.2% (by fine Gaussian SVM) to 66.8 % (by Quadratic SVM). Moreover, our work indicates that the selection of these predictors has to be performed at each spatial resolution. Indeed, the determination of Lau Basin as the origin of a specimen can be performed using our Quadratic SVM model with 7 predictors (**Fig. 6b**), but only two predictors were required to identify the site of origin within the Lau Basin (**Fig. 7a**), with a much better success rate.

In most cases here, SVM appeared to generate the best model. Dixon & Brereton (2009) explored different model types from various datasets and concluded that SVM generally provide better results than other methods when data normality is not achieved, which is the case here. Linear discriminant analysis, the most commonly used classification method in the literature, was selected as an appropriate method for only one of the seven models presented in this work, for a dataset that presented classes with well-separated distributions (**Fig. 7a**; **Supplementary Information 5**). Our success rates of elemental fingerprints appeared to be similar to or better than those of models from coastal environments in the literature (*e.g.*, Becker et al., 2005; Simmonds et al., 2014; Gomes et al., 2016; Ley & Rolls, 2018).

Our dataset of larval shells included at least two biosamples for over half of our sites. This strategy allowed us to note that variability of shell composition was higher at inter-site level compared to intra-site (**Supplementary Information 5**). However, it is important to note that several limitations are not taken into account here. First, temporal variations in the vent activity are undefined, and would require a long-term monitoring on site, as well as samples collected at different times in the year to address the potential impact on the elemental fingerprints. This can be of particular interest for species with a continuous reproduction, which appears to be the case for *S. tollmanni* (Poitrimol, 2022; p. 94). Also, our models include only the sites we collected samples from. Other hydrothermal sites can be present in the region that are still yet to be discovered, although the sampling in our study is substantial, with 14 hydrothermal sites, including two newly discovered vent fields (La Scala, in the Woodlark Basin: Boulart et al., 2022; and Mangatolo). For example, the work of Breusing et al. (2016) suggested the presence of yet undiscovered sites on the mid-Atlantic Ridge, based on the combination of biophysical models and population genetics. To circumvent such potential limits, which are not specific of deep-sea settings but also exist in coastal systems, Simmonds et al. (2014) suggested a kriging method that interpolates elemental fingerprints in locations where no samples were available. However, if this method is of interest in coastal environments where shell fingerprints are defined from the distance from river sources, it is not relevant here. Indeed, hydrothermal vent systems are patchy environments, separated by hundreds to thousands of kilometres of ‘regular’ seawater, and the composition of these vents cannot be interpolated. Still, our models should at least help provide the region of origin, even if the exact site is unknown. Additional samples collected from other sites will complement the models for future assignation of post-dispersal stages individuals.

The impact of upcoming deep-sea mining programs on hydrothermal population dynamics and biodiversity throughout the world will depend strongly on the connectivity of populations. Our study assessed the accuracy of elemental fingerprinting of deep-sea hydrothermal mollusc larval shells to determine the geographic origin of individuals at different spatial scales. We found that hydrothermal vent fields have sufficiently distinct chemistry that reflects in *S. tollmanni* larval shells to identify the origin of an individual with an accuracy ranging from 70 to 100% across 3,000 km in the South-western Pacific Ocean. Most accurate assignation models correspond to geographically-restricted regions of vent fields, and require less predictors. This implies that if larval dispersal potential is known to be restricted to a few hundreds of kilometres by other means (such as biophysical models or population genetics), the determination of the origin of specimens will be easier to perform and more precise. The next step that needs to be taken now is to analyse the pre-dispersal shell of juveniles after they have settled. With this method, it will be possible to examine the proportion of self-recruitment on any site, and determine the origin of migrants to study the connectivity and the ability for a population to recover after perturbations. These information will be of utmost importance to understand the potential impacts of deep-sea mining ventures.

METHODS

Sampling

Shinkailepas tollmanni egg capsules are abundant in ridges and folds on the shell surface of the large provannid gastropod *Ifremeria nautilei*. We collected *I. nautilei* individuals during the oceanographic cruise CHUBACARC (Hourdez & Jollivet, 2019) aboard the research vessel *L'Atalante* in spring 2019. Provannid gastropods were collected using the remotely operated vehicle (ROV) VICTOR 6000, and their shells were examined for *S. tollmanni* egg capsules using a binocular microscope within hours of collection. As *I. nautilei* individuals were collected in collection boxes that were closed before surfacing, we used the deep sea water contained in these boxes to fill the crevices of the *I. nautilei* shells containing the capsules to be opened, and then recovered larvae that had reached the veliger stage (swimming larvae with visible shell). All material was washed with nitric acid and rinsed with pure water before use. After collection, the larvae were stored dry at -20°C in groups of 10 to 100 in 2 mL eppendorfs until processed according to the protocol described below.

Habitat seawater composition analysis

Habitat seawater chemical composition measurements were performed immediately above the *Ifremeria* communities at the sites using an *In-Situ Fluid Sampler* (PIF) manipulated by the ROV arm. Not all sites explored comprised *S. tollmanni*, but where there were, habitat seawater was measured at the exact location of the biosamples prior collection.

Larval shell preparation

Details of the sample preparation are described at Protocols.io (Mouchi et al., 2022). All materials handled in the cleaning and preparation of the samples were acid-cleaned using 10% PrimarPlus-Trace analysis grade HNO_3 and rinsed with ultrapure water. All work was performed in a clean lab under a laminar flow cabinet (ISO5). No metallic objects were used in contact of the samples at any stage of the sample cleaning. To remove the soft body from the shells, we used a protocol modified from Becker et al. (2005). A solution of Optima-grade H_2O_2 at 30% was buffered with 0.05 $mol.L^{-1}$ NaOH (Suprapur) to obtain a pH of 8.5. The final H_2O_2 concentration was approximately 15%. Larvae were placed in a glass container with the H_2O_2 solution overnight, then rinsed with ultrapure water and collected by a sable brush to place them on an Extra Pure carbon adhesive tabs (Science Services) on a microscope slide. After the remaining ultrapure water dried out on the tabs, the slides were placed in a clean airtight plastic box until analysis.

Individual larval shell geochemistry analysis

The elemental composition of cleaned larval shells was measured at the Institut des Sciences Analytiques et de Physico-Chimie pour l'Environnement et les Matériaux, Université de Pau et des Pays de l'Adour, with an Agilent 8900 ICP-MS Triple Quad coupled with a femtosecond laser ablation system. The laser system was set to generate pulses of 23 $\mu J.cm^{-2}$ at 50 Hz. Each shell was ablated with these parameters, while the laser beam was continuously moved (1 $mm.s^{-1}$) due to a 2D galvanometric scanner following the trajectory of a disc of 100 µm diameter. For each acquisition, the disc was performed twice to ensure the total ablation of the larval shell, but not more to prevent the ablation of the tape. Measured elements were Mg, Cr, Mn, Fe, Cu, Zn, As, Sr, Cd, Sn, Sb, Ba, Pb and Ca as the internal standard to control the ablated volume. Calibration was performed by the successive measurements of the reference materials NIST SRM 610, 612 and 614 at the beginning, the middle and the end of each analytical session. Data reduction was performed using an in-lab developed software FOCAL 2.41. Accuracy of the measurements were checked by measuring the otolith certified reference materials (CRM) FEBS-1 and NIES-22 against the preferred values from the GeoRem database (Jochum et al., 2005), when available.

Data processing

All data processing was performed using the Matlab software (Mathworks, www.mathworks.com, v. R2022a). For shells, most elements did not exhibit a normal distribution for each site, even after transformation (Kolmogorov-Smirnov tests), which prevents the use of MANOVA. In order to facilitate interpretation of PCA and classifications, all measurements were transformed to the cubic root (Chen & Deo, 2004) to improve the dispersion of data. Classification models were performed using the Matlab ClassificationLearner application and five equal folds of the dataset for cross-validation: each fold was successively used as validation fold to assess the model based on the remaining four folds, and a mean classification rate was calculated from the five validation folds. A total of 31 model types (available in ClassificationLearner) were tested to identify, for each dataset (total, Manus-Woodlark, East-Woodlark, and regions in the Eastern domain), the model type presenting the best assignation success rate. The quality of all selected models was assessed by randomization using a modified version of the Matlab code (**Supplementary Information 6**) by White & Ruttenberg (2007), which was initially restricted to discriminant analysis. Due to computing time, the model considering all 14 sites was randomized 500 times (over 20 days of computing). All other models were randomized 1000 times.

ACKNOWLEDGEMENTS

This research was carried out under the ANR CERBERUS project (ANR-17-CE02-0003). We would like to thank the captain and crew of the French Research Vessel *L'Atalante* and the team in charge of the ROV 6000 Victor, without whom sampling would not have been possible. Ship time was supported by the French Oceanographic Fleet (Hourdez & Jolliver, 2019).

REFERENCES

Amon, D.J., Gollner, S., Morato, T., Smith, C.R., Chen, C., Christiansen, S., Currie, B., Drazen, J.C., Fukushima, T., Gianni, M., Gjerde, K.M., Gooday, A.J., Guillen Grillo, G., Haeckel, M., Joyini, T., Ju, S.-J., Levin, L.A., Metaxas, A., Mianowicz, K., Molodtsova, T.N., Narberhaus, I., Orcutt, B.N., Swaddling, A., Tuhumwire, J., Urueña Palacio, P., Walker, M., Weaver, P., Xu, X.-W., Mulalap, C. Y., Edwards, P.E.T., Pickens, C., 2022. Assessment of scientific gaps related to the effective environmental management of deep-seabed mining. *Marine Policy,* 138, 105006. doi: 10.1016/j.marpol.2022.105006.

Baco, A., Etter, R.J., Ribeiro, P.A., von der Heyden, S., Beerli, P., Kinlan, B.P., 2016. A synthesis of genetic connectivity in deep-sea fauna and implications for marine reserve design.

Molecular Ecology, 25, 3276–3298. doi: 10.1111/mec.13689.

Becker, B.J., Fodrie, F.J., McMillan, P.A., Levin, L.A., 2005. Spatial and temporal variation in trace elemental fingerprints of mytilid mussel shells: a precursor to invertebrate larval tracking. *Limnology and Oceanography*, 50, 48-61. doi: 10.4319/lo.2005.50.1.0048.

Becker, B.J., Levin, L.A., Fodrie, F.J., McMillan, P.A., 2007. Complex larval connectivity patterns among marine invertebrate populations. *Proceedings of the National Academy of Sciences*, 104, 3267-3272. doi: 10.1073/pnas.0611651104.

Boschen, R.E., Rowden, A.A., Clark, M.R., Gardner, J.P.A., 2013. Mining of deep-sea seafloor massive sulfides: A review of the deposits, their benthic communities, impacts from mining, regulatory frameworks, and management strategies. *Ocean & Coastal Management*, 84, 54-67. doi: 10.1016/j.ocecoaman.2013.07.005.

Bouchoucha, M., Pécheyran, C., Gonzales, J.L., Lenfant, P., Darnaude, A.M., 2018. Otolith fingerprints as natural tags to identify juvenile fish life in ports. *Estuarine, Coastal and Shelf Science*, 212, 210-218. doi: 10.1016/j.ecss.2018.07.008.

Boulart, C., Rouxel, O., Scalabrin, C., Le Meur, P., Pelleter, E., Poitrimol, C., Thiébaut, E., Matabos, M., Castel, J., Tran Lu Y, A., Michel, L.N., Cathalot, C., Chéron, S., Boissier, A., Germain, Y., Guyader, V., Arnaud-Haond, S., Bonhomme, F., Broquet, T., Cueff-Gauchard, V., Le Layec, V., L'Haridon, S., Mary, J., Le Port, A.S., Tasiemski, A., Kuama, D.C., Hourdez, S., Jollivet, D., 2022. Active hydrothermal vents in the Woodlark Basin may act as dispersing centres for hydrothermal fauna. *Communications Earth & Environment*, 3, 64. doi: 10.1038/s43247-022-00387-9.

Bounket, B., Tabouret, H., Gibert, P., Bareille, G., Pécheyran, C., Carrel, G., Argillier, C., Morat, F., 2021. Spawning areas and migration patterns in the early life history of *Squalius cephalus* (Linnaeus, 1758): Use of otolith microchemistry for conservation and sustainable management. *Aquatic Conservation: Marine and Freshwater Ecosystems*, 31, 2772-2787. doi: 10.1002/aqc.3682.

Breusing, C., Biastoch, A., Drews, A., Metaxas, A., Jollivet, D., et al., 2016. Biophysical and population genetic models predict the presence of "Phantom" stepping stones connecting mid-Atlantic ridge vent ecosystems. Current Biology 26, 2257-2267. doi: 10.1016/j.cub.2016.06.062.

Carson, H.S., 2010. Population connectivity of the Olympia oyster in Southern California. *Limnology and Oceanography*, 55, 134-148. doi: 10.4319/lo.2010.55.1.0134.

Castel, J., Hourdez, S., Pradillon, F., Daguin-Thiébaut, C., Ballenghien, M., Ruault, S., Corre, E., Tran Lu Y, A., Mary, J., Gagnaire, P.A., Bonhomme, F., Breusing, C., Broquet, T., Jollivet, D., 2022. Inter-specific genetic exchange despite strong divergence in deep-sea hydrothermal vent gastropods of the genus *Alviniconcha*. *Genes*, 13, 985. doi: 10.3390/genes13060985.

Chen, W.W., Deo, R.S., 2004. Power transformations to induce normality and their applications.

Journal of the Royal Statistical Society: Series B, 66, 117-130. doi: 10.1111/j.1467-9868.2004.00435.x.

Christiansen, S., Bräger, S., Jaeckel, A., 2022. Evaluating the quality of environmental baselines for deep seabed mining. *Frontiers in Marine Science*, 9, 898711. doi: 10.3389/fmars.2022.898711

Cunha, M.R., Génio, L., Pradillon, F., Clavel Henry, M., Beaulieu, S., Birch, J., Campuzano, F.J., Carretón, M., De Leo, F., Gula, J., Laming, S., Lindsay, D., Matos, F.L., Metaxas, A., Meyer-Kaiser, K0, Mills, S., Queiroga, H., Rodrigues, C.F., Sarrazin, J., Watanabe, H., Young, R., Young, C.M., 2020. Foresight Workshop on Advances in Ocean Biological Observations: a sustained system for deep-ocean meroplankton. *Research Ideas and Outcomes*, 6, e54284. doi: 10.3897/rio.6.e54284.

Danovaro, R., Aguzzi, J., Fanelli, E., Billett, D., Gjerde, K., Jamieson, A., Ramirez-Llodra, E., Smith, C.R., Snelgrove, P.V.R., Thomsen, L., Van Dover, C.L., 2017. An ecosystem-based deep-ocean strategy. *Science*, 355, 452-454. doi: 10.1126/science.aah7178.

Danovaro, R., Fanelli, E., Aguzzi, J., Billett, D., Carugati, L., Corinaldesi, C., Dell'Anno, A., Gjerde, K., Jamieson, A.J., Kark, S., McClain, C., Levin, L., Levin, N., Ramirez-Llodra, E., Ruhl, H., Smith, C.R., Snelgrove, P.V.R., Thomsen, L., Van Dover, C.L., Yasuhara, M., 2020. Ecological variables for developing a global deep-ocean monitoring and conservation strategy. *Nature Ecology & Evolution*, 4, 181-192. doi: 10.1038/s41559-019-1091-z.

DePaolo, D.J., 2011. Surface kinetic model for isotopic and trace element fractionation during precipitation of calcite from aqueous solutions. *Geochimica et Cosmochimica Acta*, 416, 67-72. doi: 10.1016/j.gca.2010.11.020.

Dixon, S.J., Brereton, R.G., 2009. Comparison of performance of five common classifiers represented as boundary methods: Euclidean Distance to Centroids, Linear Discriminant Analysis, Quadratic Discriminant Analysis, Learning Vector Quantization and Support Vector Machines, as dependent on data structure. *Chemometrics and Intelligent Laboratory Systems*, 95, 1-17. doi: 10.1016/j.chemolab.2008.07.010.

Dunn, D.C., Van Dover, C.L., Etter, R.J., Smith, C.R., Levin, L.A., Morato, T., Colaço, A., Dale, A.C., Gebruk, A.V., Gjerde, K.M., Halpin, P.N., Howell, K.L., Johnson, D., Perez, J.A.A., Ribeiro, M.C., Stuckas, H., Weaver, P., SEMPIA Workshop Participants, 2018. A strategy for the conservation of biodiversity on mid-ocean ridges from deep-sea mining. *Science Advances*, 4, eaar4313. doi: 10.1126/sciadv.aar4313.

Fodrie, F.J., Becker, B.J., Levin, L.A., Gruenthal, K., McMillan, P.A., 2011. Connectivity clues from short-term variability in settlement and geochemical tags of mytilid mussels. *Journal of Sea Research*, 65, 141-150. doi: 10.1016/j.seares.2010.09.001.

Fouquet, Y., Von Stackelberg, U., Charlou, J.L., Donval, J.P., Erzinger, J., Foucher, J.P., Herzig, P., Mühe, R., Soakai, S., Wiedicke, M., Whitechurch, H., 1991. Hydrothermal activity and metallogenesis in the Lau back-arc basin. *Nature*, 349, 778-781. doi: 10.1038/349778a0.

Fouquet, Y., Pelleter, E., Konn, C., Chazot, G., Dupré, S., Alix, A.S., Chéron, S., Donval, J.P., Guyader, V., Etoubleau, J., Charlou, J.L., Labanieh, S., Scalabrin, C., 2018. Volcanic and hydrothermal processes in submarine calderas: the Kulo Lasi example (SW Pacific). *Ore Geology Reviews*, 99, 314-343. doi: 10.1016/j.oregeorev.2018.06.006.

Gagnaire, P.-A., Broquet, T., Aurelle, D., Viard, F., Souissi, A., Bonhomme, F., Arnaud-Haond, S., Bierne, N., 2015. Using neutral, selected, and hitchhiker loci to assess connectivity of marine populations in the genomic era. *Evolutionary Applications*, 8, 769-786. doi:10.1111/eva.12288.

Gollner, S., Kaiser, S., Menzel, L., Jones, D.O.B., Brown, A., Mestre, N.C., van Oevelen, D., Menot, L., Colaço, A., Canals, M., Cuvelier, D., Durden, J.M., Gebruk, A., Egho, G.A., Haeckel, M., Marcon, Y., Mevenkamp, L., Morato, T., Pham, C.K., Purser, A., Sanchez-Vidal, A., Vanreusel, A., Vink, A., Martinez Arbizu, P., 2017. Resilience of benthic deep-sea fauna to mining activities. *Marine Environmental Research*, 129, 76-101. doi: 10.1016/j.marenvres.2017.04.010.

Gwyther, D., 2008. Environmental impact statement, Solwara 1 project, Vol A. Nautilus Minerals Niugini Limited. Coffey Natural Systems, Brisbane.

Honig, A., Etter, R., Pepperman, K., Morello, S., Hannigan, R., 2020. Site and age discrimination using trace element fingerprints in the blue mussel, *Mytilus edulis*. *Journal of Experimental Marine Biology and Ecology*, 522, 151249. doi: 10.1016/j.jembe.2019.151249.

Hourdez, S., Jollivet, D., 2019. CHUBACARC cruise, *L'Atalante R/V*. doi: 10.17600/18001111.

Jochum, K.P., Nohl, U., Herwig, K., Lammel, E., Stoll, B., Hofmann, A.W., 2005. GeoReM: A new Geochemical database for reference materials and isotopic standards. *Geostandards and Geoanalytical Research*, 29, 333-338, doi 10.1111/j.1751-908X.2005.tb00904.x.

Jouffray, J.-B., Blasiak, R., Norström, A.V., Österblom, H., Nyström, M., 2020. The blue acceleration: the trajectory of human expansion into the ocean. *One Earth*, 2, 43-54. doi: 10.1016/j.oneear.2019.12.016

Konn, C., Donval, J. P., Guyader, V., Roussel, E., Fourré, E., Jean-Baptiste, P., Pelleter, E., Charlou, J. L., Fouquet, Y., 2018. Organic, gas, and element geochemistry of hydrothermal fluids of the newly discovered extensive hydrothermal area in the Wallis and Futuna region (SW Pacific). *Geofluids*, 7692839. doi: 10.1155/2018/7692839.

Kroll, I.R., Poray, A.K., Puckett, B.J., Eggleston, D.B., Fodrie, F.J., 2016. Environmental effects on elemental signatures in eastern oyster *Crassostrea virginica* shells: using geochemical tagging to assess population connectivity. *Marine Ecology Progress Series*, 543, 173-186. doi: 10.3354/meps11549.

Lee, J.G., Roberts, S.B., Morel, F.M.M., 1995. Cadmium: a nutrient for the marine diatom *Thalassiosira weissflogii*. *Limology and Oceanography*, 40 1056-1063. doi: 10.4319/lo.1995.40.6.1056.

Levin, L.A., 1990. A review of methods for labeling and tracking marine invertebrate larvae. *Ophelia*, 32, 115-144. doi: 10.1080/00785236.1990.10422028.

Levin, L.A., Huggett, D., Myers, P., Bridges, T., Weaver, J., 1993. Rare-earth tagging methods for the study of larval dispersal by marine invertebrates. *Limnology and Oceanography*, 38, 346-360. doi: 10.4319/lo.1993.38.2.0346.

Ley, J.A., Rolls, H.J., 2018. Using otolith microchemistry to assess nursery habitat contribution and function at a fine spatial scale. *Marine Ecology Progress Series*, 606, 151-173. doi: 10.3354/meps12765.

McVeigh, D.M., Eggleston, D.B., Todd, A.C., Young, C.M., He, R., 2017. The influence of larval migration and dispersal depth on potential larval trajectories of a deep-sea bivalve. *Deep-Sea Research I*, 127, 57-64. doi: 10.1016/j.dsr.2017.08.002.

Miller, K.A., Thompson, K.F., Johnston, P., Santillo, D., 2018. An overview of seabed mining including the current state of development, environmental impacts, and knowledge gaps. *Frontiers in Marine Science*, 4, 418. doi: 10.3389/fmars.2017.00418.

Mitarai, S., Watanabe, H., Nakajima, Y., Shchepetkin, A.F., McWilliams, J.C., 2016. Quantifying dispersal from hydrothermal vent fields in the western Pacific Ocean. *Proceedings of the National Academy of Science*, 113, 2976-2981. doi: 10.1073/pnas.1518395113.

Mercier, L., Darnaude, A.M., Bruguier, O., Vasconcelos, R.P., Cabral, H.N., Costa, M.J., Lara, M., Jones, D.L., Mouillot, D., 2011. Selecting statistical models and variable combinations for optimal classification using otolith microchemistry. *Ecological Applications*, 21, 1352–1364. doi: 10.1890/09-1887.1.

Mouchi, V., Godbillot, C., Forest, V., Ulyanov, A., Lartaud, F., de Rafélis, M., Emmanuel, L., Verrecchia, E.P., 2020. Rare Earth Elements in oyster shells: provenance discrimination and potential vital effects. *Biogeosciences*, 17, 2205-2217. doi: 10.5194/bg-17-2205-2020.

Mouchi, V., Broquet, T., Comtet, T., 2022. Preparation of mollusc larval shells for individual geochemical analysis. *Protocols.io*. doi: 10.17504/protocols.io.bp2l61jwkvqe/v1.

Podowski, E.L., Ma, S., Luther III, G.W., Wardrop, D., Fisher, C.R., 2010. Biotic and abiotic factors affecting distributions of megafauna in diffuse flow on andesite and basalt along the Eastern Lau Spreading Center, Tonga. *Marine Ecology Progress Series*, 418, 25-45. doi: 10.3354/meps08797.

Pol, A., Barends, T.R.M., Dietl, A., Khadem, A.F., Eygensteyn, J., Jetten, M.S.M., Op den Camp, H.J.M., 2014. Rare earth metals are essential for methanotrophic life in volcanic mudpots. *Environmental Microbiology*, 16, 255-264. doi: 10.1111/1462-2920.12249.

Poitrimol, C., 2022. Distribution et partitionnement de la biodiversité hydrothermale dans un système discontinu de dorsales : le cas des bassins arrière-arc de l'ouest Pacifique. *Ph.D. thesis* at Sorbonne Université, 270 p.

Poitrimol, C., Thiébaut, E., Daguin-Thiébaut, C., Le Port, A.S., Ballenghien, M., Tran Lu Y, A., Jollivet, D., Hourdez, S., Matabos, M., 2022. Contrasted phylogeographic patterns of hydrothermal vent gastropods along South West Pacific: Woodlark Basin, a possible contact zone and/or stepping-stone. *PLoS ONE*, 17, e0275638. doi: 10.1371/journal.pone.0275638.

Ramesh, K., Hu, M.Y., Thomsen, J., Bleich, M., Melzner, F., 2017. Mussel larvae modify calcifying fluid carbonate chemistry to promote calcification. *Nature Communications*, 8, 1709. doi: 10.1038/s41467-017-01806-8.

Simmonds, S.E., Kinlan, B.P., White, C., Paradis, G.L., Warner, R.R., Zacherl, D.C., 2014. Geospatial statistics strengthen the ability of natural geochemical tags to estimate range-wide population connectivity in marine species. *Marine Ecology Progress Series*, 508, 33-51. doi: 10.3354/meps10871.

Smith, C.R., Tunnicliffe, V., Colaço, A., Drazen, J.C., Gollner, S., Levin, L.A., Mestre, N.C., Metaxas, A., Molodtsova, T.N., Morato, T., Sweetman, A.K., Washburn, T., Amon, D.J., 2020. Deep-sea misconceptions cause underestimation of seabed-mining impacts. *Trends in Ecology and Evolution*, 35, 853-857. doi: 10.1016/j.tree.2020.07.002.

Suzuki, K., Yoshida, K., Watanabe, H., Yamamoto, H., 2018. Mapping the resilience of chemosynthetic communities in hydrothermal vent fields. *Scientific Reports*, 8, 9364. doi: 10.1038/s41598-018-27596-7.

Thorrold, S.R., Zacherl, D.C., Levin, L.A., 2007. Population connectivity and larval dispersal using geochemical signatures in calcified structures. *Oceanography*, 20, 80-89.

Tran Lu Y, A., 2022. La phylogéographie comparée d'espèces hydrothermales du Pacifique Ouest à l'heure de la génomique des populations. *Ph.D. thesis* at Université de Montpellier, 244 p.

Tran Lu Y, A., Ruault, S., Daguin-Thiébaut, C., Castel, J., Bierne, N., Broquet, T., Wincker, P., Perdereau, A., Arnaud-Haond, S., Gagnaire, P.A., Jollivet, D., Hourdez, S., Bonhomme, F., 2022. Subtle limits to connectivity revealed by outlier loci within two divergent metapopulations of the deep-sea hydrothermal gastropod *Ifremeria nautilei*. *Molecular Ecology*, 31, 2796-2813. doi: 10.1111/mec.16430.

Ulrich, R.N., Guillermic, M., Campbell, J., Hakim, A., Han, R., Singh, S., Stewart, J.D., Román-Palacios, C., Carroll, H.M., De Corte, I., Gilmore, R.E., Doss, W., Tripati, A., Ries, J.B., Eagle, R.A.,

2021. Patterns of element incorporation in calcium carbonate biominerals recapitulate phylogeny for a diverse range of marine calcifiers. *Frontiers in Earth Sciences*, 9, 641760. doi: 10.3389/feart.2021.641760.

Van Dover, C.L., 2014. Impacts of anthropogenic disturbances at deep-sea hydrothermal vent ecosystems: a review. *Marine Environmental Research*, 102, 59-72. doi: 10.1016/j.marenvres.2014.03.008.

Watson, E.B., 2004. A conceptual model for near-surface kinetic controls on the trace-element and stable isotope composition of abiogenic calcite crystals. *Geochimica et Cosmochimica Acta*, 68, 1473-1488. doi: 10.1016/j.gca.2003.10.003.

Weiner, S., Dove, P.M., 2003. An overview of biomineralization processes and the problem of the vital effect. *Reviews in Mineralogy and Geochemistry*, 54, 1-29. doi: 10.2113/0540001.

White, J.W., Ruttenberg, B.I., 2007. Discriminant function analysis in marine ecology: some oversights and their solutions. *Marine Ecology Progress Series*, 329, 301-305. doi: 10.3354/meps329301.

Yearsley, J.M., Salmanidou, D.M., Carlsson, J., Burns, D., Van Dover, C.L., 2020. Biophysical models of persistent connectivity and barriers on the northern Mid-Atlantic Ridge. *Deep-Sea Research II*, 180, 104819. doi: 10.1016/j.dsr2.2020.104819.

Zacherl, D.C., Manríquez, P.H., Paradis, G., Day, R.W., Castilla, J.C., Warner, R.R., Lea, D.W., Gaines, S.D., 2003. Trace elemental fingerprinting of gastropod statoliths to study larval dispersal trajectories. *Marine Ecology Progress Series*, 248, 297-303. doi:10.3354/meps248297.